Molecular Dynamics Study of the Thermal Behavior of Nanometer-Sized Au Hollow Cubes

Francesco Delogu*

Dipartimento di Ingegneria Chimica e Materiali, Università degli Studi di Cagliari, piazza d'Armi, I-09123 Cagliari, Italy

Received: September 26, 2007; In Final Form: November 21, 2007

Molecular dynamics simulations have been employed to study the thermal response of an Au hollow cube with a side about 8 nm long and walls about 3 nm thick. The gradual temperature rise determines the occurrence of a hierarchical sequence of melting transitions regarding atoms with a progressively increasing number of nearest neighbors. Atoms located at the cube edges are thus seen to undergo melting first, then followed by surface and grain boundary species, and finally by atoms in bulklike regions of cube walls. A percolating liquidlike framework connecting external and internal surfaces is formed in the temperature range within which grain boundaries are partially molten. Such framework represents a preferential diffusion path for liquidlike species.

Introduction

Nanometer-sized structures with a hollow interior can in principle find useful application in many areas of fundamental and applied research.[1,2] They can be for example employed as encapsulating containers in related fields such as heterogeneous catalysis, drug delivery, and protection of chemicals from damaging environment.[1−4] Among the others, noble metal hollow nanostructures have attracted particular interest because of their plasmonic properties in the UV−visible spectral region. Unlike nanoparticles even of the same metal, hollow systems exhibit indeed strong scattering and absorption peaks in the near-infrared region with important consequences on their photothermal response.[1,5]

Hollow spheres of various metals, oxides, and nitrides have been synthesized by templating against nanometer-sized colloid particles.[6−9] The external surfaces of template systems are typically coated with thin layers of desired materials to form core/shell particles, and templates are successively removed. In the case of metals, synthetic methods[10−12] lead to nanoshells with polycrystalline walls characterized by weak mechanical strength. A recently developed approach based on so-called template-engaged replacement reactions permits however the generation of hollow nanostructures with regular geometry, void spaces, and highly crystalline walls.[13−16] Extended from Ag, Au, and Pd to other materials,[17−21] the method allows for example the preparation of hollow nanocubes with well-defined surface plasmon resonance.

Despite their promising properties, a detailed knowledge of the thermodynamic behavior of hollow nanosystems is currently lacking. Only a few theoretical studies dealt in fact with hollow particles on the nanoscale,[22] whereas much more analyzed has been the behavior of nanotubes.[23−28] To partially fill such a gap, the present work focuses on the thermal properties of a nanometer-sized Au hollow cube formed by six equivalent crystalline walls with (100) crystallographic facets separated by grain boundary (GB) regions. Element and geometry have not been arbitrarily chosen. Cubic Au nanoshells can be indeed synthesized in solution by templating over Ag nanocubes.[14] This opens the door to an experimental confirmation of numerical findings which is particularly desirable in the present case. Molecular dynamics (MD) calculations predict indeed the occurrence, under suitable circumstances, of unexpected and potentially useful atomic-scale diffusion processes allowing atomic species to move from inner to outer surfaces and vice versa across GBs.

Numerical Simulations

The nanometer-sized hollow cube was generated by modifying the methodology generally employed to obtain nanocrystalline structures with randomly oriented grains.[29] In the present case neighboring domains were indeed oriented to produce the desired cubic symmetry with (100) crystallographic facets. Six *cF*4 face-centered cubic (fcc) domains were constructed starting from six different locations until there was overlap between neighboring lattices. Whenever two atoms were found at distances smaller than 2 Å, one of them was selected and removed. Square domains approximately 8 nm long and 3 nm thick were considered, each consisting of about 4960 atoms.

Interatomic forces were reproduced by a semiempirical potential based on the second-moment approximation of tight-binding (TB) band energy.[30] The cohesive energy

$$E = \sum_{i=1}^{N} \left\{ \sum_{j=1}^{N} A e^{-p((r_{ij}/r_0)-1)} - \left[\sum_{j=1}^{N} \xi^2 e^{-2q((r_{ij}/r_0)-1)} \right]^{1/2} \right\} \quad (1)$$

depends on the distance r_0 of nearest neighbors at 0 K, on the distance $r_{ij} = |r_i - r_j|$ between atoms i and j, and on characteristic potential parameters A, ξ, p, and q reported in Table 1.[30] Interactions were computed within a cutoff radius extending approximately to seventh neighbors. Equations of motion were solved with a fifth-order predictor-corrector algorithm[31] and a time step of 2.0 fs. Calculations were carried out in the *NhT* ensemble with number of atoms N, shape h, and temperature T constant.[32] Undesired dynamical processes due to the undamped collective motion of atomic planes parallel to free surfaces were avoided by relaxing the initial atomic configuration at 300 K for 200 ps and then at 600 K for

* Corresponding author e-mail: delogu@dicm.unica.it.

10.1021/jp077713p CCC: $40.75
Published on Web 02/21/2008

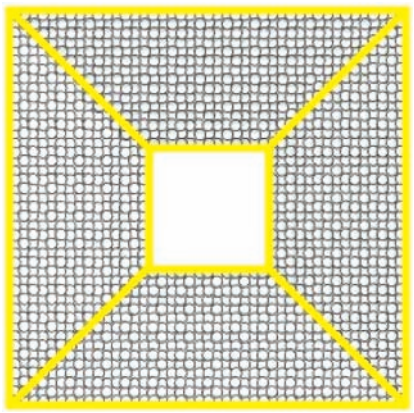

Figure 1. A cross section of the equilibrated nanometer-sized hollow cube at 600 K. Thick lines are superposed to point out the arrangement of lateral walls. A cross-sectioned layer about 0.5 nm thick is reported.

TABLE 1: TB Potential Parameters for Au[30]

A, kJ mol^{-1}	19.886
ξ, kJ mol^{-1}	172.714
p	10.229
q	4.036
r_0, Å	2.884

additional 200 ps. Relaxation took place via short-range atomic displacements accommodating local atomic strains due to the distortion of coordination shells. The relatively low-temperature greatly limited the extent of atomic disordering processes, which mostly involved surface and GB atoms due to their defective coordination. A cross section of the equilibrated nanometer-sized hollow cube at 600 K is reported in Figure 1.

Starting from 600 K, the system temperature was slowly raised 2 K every 20 ps. Any temperature increase determined a corresponding increase of the amplitude of atomic vibrations around equilibrium lattice sites. For each atom, the extent of such an increase was strictly dependent on the local arrangement of its nearest neighbors.[33,34] Possessing different coordination shells, atoms located at edges, free surfaces, GBs, and in the interior of coherent crystalline domains exhibited different thermal responses.

GB regions deserve a short comment. Each crystalline wall was constructed by starting from a position in the three-dimensional space randomly selected within the suitable ranges of Cartesian coordinates. Experimental evidence suggests indeed that epitaxial relationships connect templating surfaces with hollow structure walls.[13−16] Coherent crystalline walls of experimentally obtained hollow structures are thus thought to nucleate at random on template surface sites. Under such conditions, no rigid constraint promotes the formation of equal GB structures, although twin faults should be expected.[13−16] It should be also noted that the relatively high-temperature range here explored does not allow any simple characterization of the GB structure. Initial GB atomic configurations can be roughly assimilated to (110)×(110) twin boundaries. Local atomic strain relaxation and thermalization processes determine however further disordering.

Aimed at properly characterizing the melting behavior and distinguishing between solid- and liquidlike dynamics, a local order parameter depending on the symmetry of coordination shell was defined for each atomic species. Following previous work,[33,34] a set of N_q wave vectors $\boldsymbol{q}$ such that $e^{i\boldsymbol{q}\cdot\boldsymbol{r}} = 1$ was selected for any vector $\boldsymbol{r}$ connecting a pair of opposite nearest neighbors in a perfect fcc lattice. Only one of the two identical antiparallel $\boldsymbol{r}$ vectors connecting any given atom pair was considered. N_q amounted then to 6. The local order parameter was defined as

$$\psi_i = \left| \frac{1}{N_q z} \sum_{\mathrm{r}} \sum_{\mathrm{q}} e^{iq\cdot r} \right|^2 \tag{2}$$

where the sum on $\boldsymbol{r}$ vectors runs over the z nearest neighbors of atom i. Nearest neighbors are here defined as any two atoms located at distances smaller than the one, $r_{\min}$, at which the pair correlation function[31] has its first minimum. ψ_i is equal to 1 for any atom in a perfect fcc lattice site and smaller otherwise.[33,34] The discrimination between atoms with dynamic features typical of solid or liquid phase is considerably improved when suitably averaged atomic positions are used and the degree of order of nearest neighbors accounted for. Instantaneous atomic positions are indeed affected by fast thermal vibrations which decrease the instantaneous degree of order of a given atomic configuration. ψ_i was therefore evaluated on atomic positions averaged over 15 ps, and an average local order parameter

$$\bar{\psi}_i = \frac{1}{z+1}(\psi_i + \sum_j \psi_j) \tag{3}$$

was defined,[33,34] j running over the z nearest neighbors of the atom i. According to the literature,[33,34] atoms in a liquid region are characterized by $\bar{\psi}_i$ values smaller than 0.05, whereas the solid phase includes atomic species with $\bar{\psi}_i$ values larger than 0.2. It is here worth noting that the choice of $\bar{\psi}_i$ threshold values can in principle affect the final results of dynamical analysis. Selecting a suitable $\bar{\psi}_i$ threshold is therefore crucial to properly characterize the atomic-scale dynamics. The number of atoms with a dynamic behavior intermediate between liquid and solid is however so small that using a single $\bar{\psi}_i$ threshold does not introduce approximations able to change the framework of results.[33,34] The threshold was set at 0.08. The atoms with $\bar{\psi}_i$ values smaller and larger than 0.08 will be then referred to as liquid- and solidlike, respectively.

For the sake of comparison, numerical simulations were also performed on a nanometer-sized hollow cube with walls about 8 nm long and 3 nm thick but no GB separating the lateral domains, generated by removing the atomic species located in the interior of a full single cubic crystal. It is then a single-crystal hollow cube. For the sake of clarity and brevity, the results concerning this system will not be reported. They are indeed perfectly coincident with the ones concerning the hollow cube containing GB regions, except of course the ones connected with the presence of GBs themselves. Thermal responses of cube edges and surfaces are therefore the same.

The melting point of the Au nanometer-sized hollow cube will be compared not only with the melting point of the single-crystal hollow cube but also with the Au equilibrium melting point $T_{\mathrm{m,eq}}$ characteristic of the interatomic potential used. Such a melting point roughly corresponds to the temperature at which a semicrystal terminating with a free plane surface melts.[35−40] Calculations on Au systems containing 13 500 atoms and terminating with a (100) plane surface, carried out under the same conditions adopted to study the melting behavior of the nanometer-sized hollow cube, indicate that $T_{\mathrm{m,eq}} \approx 1210$ K.[39,41,42]

Additional simulations have been also carried out to investigate the extent to which the functional form of the selected many-body interatomic potential qualitatively and quantitatively affects the system thermal response. To this end, the embedded-

atom method (EAM) potential for Au was employed.[43,44] Analyses were restricted to the number n_l of liquidlike atoms as a function of temperature T. The equilibrium melting point $T_{m,eq}$ for the EAM potential employed was estimated as discussed above. A value of about 1168 K was found, which even represents an improvement compared to previous EAM heterogeneous melting point estimates for Au.[44] Such a good performance can be reasonably ascribed to the procedure followed to produce a well relaxed plane surface, which also resulted in improved performances for the TB force scheme as described elsewhere.[39,41,42] The smaller $T_{m,eq}$ value obtained with the EAM potential compared to the TB one suggests that the significant features of EAM hollow cube thermal response should be shifted at lower temperatures. A quantitative change of characteristic temperatures for any given thermal process is therefore expected. Quantitative changes do not imply however qualitative changes in the mechanisms of thermal response. This point will be explicitly addressed when necessary in the following.

Melting Behavior

Similar to what was observed in the case of Au nanotubes,[45] the nanometer-sized hollow cube displays a relatively complex thermal response originating from the existence of sets of atoms with coordination shells differing either in the number of nearest neighbors or in their arrangement. The atoms forming the hollow cube can be indeed intuitively classified into species located at hollow structure edges, free surfaces, GBs, and bulklike interior. Possessing different coordination shells, these species are also expected to possess well distinguishable characteristic thermal properties. No reliable method is however available for an a priori classification of atoms, which has been then carried out a posteriori on the basis of the thermal properties of single atoms. Many different aspects of the melting behavior of the nanometer-sized hollow cube are similar to the ones displayed by square prism nanotubes with equal crystallographic facet and wall thickness.[45] Some details of such behavior will be therefore only briefly described in order to focus on the diffusion of atomic species. It is however also worth noting that important differences arise due to the different linear extension of GBs and the presence of vertices, which implies the formation of triple junctions. Such differences will be suitably pointed out when necessary.

The cross section of the relaxed hollow cube configuration reported in Figure 1 shows that walls are formed by sixteen (100) atomic planes. The atoms located at external edges have on the average only 3 to 6 neighbors, instead of the 9 to 11 of the internal edge ones, and possess therefore the highest potential energy. As a consequence, at any given temperature they also display the largest amplitude of vibration around their own equilibrium lattice sites. The first edge atoms with liquidlike character appear at about 850 K, and their number increases gradually with temperature in the range between 850 and 884 K. It should be noted however that even below 800 K the atoms located along the edges at the cube vertices exhibit an extremely large mobility and coordination numbers as small as 1 to 3. Their number is so small, roughly 8, that there is no practical reason to regard them separately from edge atoms. Liquidlike edge atoms possess translational degrees of freedom allowing relatively long-range displacements along the hollow cube external edges. The typical atomic trajectory reported in Figure 2 also shows that liquidlike atoms are able to move from one edge to another once they arrive to a cube vertex. The trajectory shows in addition that liquidlike edge atoms can occasionally undergo lateral displacements. In such cases, the liquidlike atom behaves like a true adatom exploring the (100) external surface. The melting process of edge atoms attains completion at 884 K.

Figure 2. A typical trajectory of a liquidlike edge atom. Thick lines mark the external edges of the hollow nanometer-sized cube. The liquidlike atom crosses the vertices of the cube and moves to an adjacent external edge. A lateral displacement on a plane free surface is also observed. Data are extracted from an atomic configuration at 864 K.

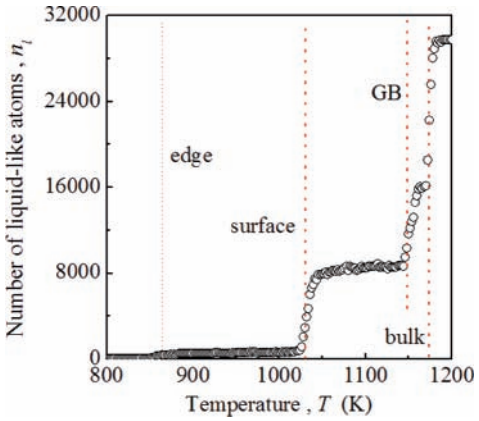

Figure 3. The number n_l of liquidlike atoms as a function of the temperature T. Four relatively marked increases are observed at about 860, 1025, 1160, and 1172 K. Each n_l rise marks the occurrence of a melting process. More specifically, the four increases point out respectively the melting of edge, surface, GB, and bulklike atoms.

Roughly between 1020 and 1030 K edge melting is followed by the solid-to-liquid transition of atoms located at the free (100) plane external and internal surfaces. This melting process has the same second-order features shown by edge atom melting but takes place on a shorter time interval. Surface melting only involves the two outer atomic planes on each side of the hollow cube crystalline walls, so that twelve planes out of the sixteen ones forming the walls keep solidlike character. These twelve planes can be therefore regarded as formed by bulklike atoms.

Edge and surface melting processes are well described by the plot of the number n_l of liquidlike atoms as a function of temperature T. Data reported in Figure 3 point out indeed two relatively marked rises at about 860 and 1025 K, followed by a less marked increase and a final transition respectively at about 1160 and 1172 K. The third rise must be ascribed to the melting

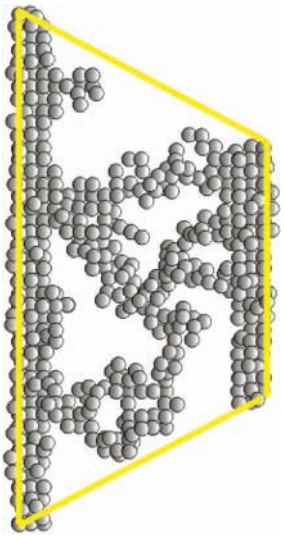

Figure 4. A snapshot of the percolating three-dimensional network of liquidlike atoms at a GB region connecting the external and the internal molten surfaces. Data refer to an atomic configuration at 1162 K.

of GB regions where, according to the average local order parameter $\bar{\psi}_i$, atoms have distorted coordination shells due to the noncompact arrangement of coordinated species and the resulting excess volume. Up to the temperature of about 1050 K the GBs separating neighboring walls are both solid and stable, and the system consists of liquidlike layers about 0.4 nm thick covering a solid core. GB melting starts above 1050 K. An increasing fraction of GB atoms displays $\bar{\psi}_i$ values below 0.08, i.e., liquidlike character, as the temperature increases in the range roughly between 1146 and 1158 K. At 1158 K approximately 30% of GB species has liquidlike character. It is here worth noting that, although the relatively small number of atoms involved does not allow a definite conclusion, most of liquidlike GB atoms appear in correspondence of triple junctions at cube vertices. As shown in detail in the following, these regions play indeed an important role in the definition of atomic mobility, which is deeply affected by the formation of liquidlike species at GBs. MD simulations 500 ps long carried out at 1158 K show that liquidlike atoms are able to move from internal to external surfaces and vice versa through the percolating liquidlike network at GBs. Clear evidence that such a network provides a three-dimensional diffusion path for liquidlike atoms is given by the liquidlike atom trajectory reported in Figure 5. GB melting attains completion at 1164 K. As already pointed out in previous work,[45] under such circumstances solidlike bulk atoms are no longer connected, and the nanometer-sized hollow cube is expected to exhibit mechanical instability when subjected to a mechanical load. A spontaneous change in shape is also expected as a consequence of clustering phenomena involving liquidlike atoms. Such processes occur however on relatively long time intervals, so that in the present simulations instability and clustering are pre-empted by the melting of bulklike atoms, which takes place at about 1172 K.

The same sequence of melting processes is observed in numerical simulations employing the EAM potential. Of course, as expected on the basis of the differences in the melting point $T_{m,eq}$ estimates worked out with TB and EAM force schemes, the temperatures at which melting processes take place are different. Differences between TB and EAM estimates are however approximately constant at about 40 K. It is interesting to note that with normalizing TB and EAM temperatures to respective melting points $T_{m,eq}$ an almost complete data superposition is observed. This is clearly illustrated in Figure 6, where the number n_l of liquidlike atoms is quoted as a function of the normalized temperature $T^* = T/T_{m,eq}$ for both TB and EAM simulations. It follows that potentials affect quantitative but not qualitative features.

Figure 5. The trajectory of a liquidlike atom diffusing from the internal to the external surface across the percolating network at GBs. Data are extracted from an atomic configuration at 1158 K.

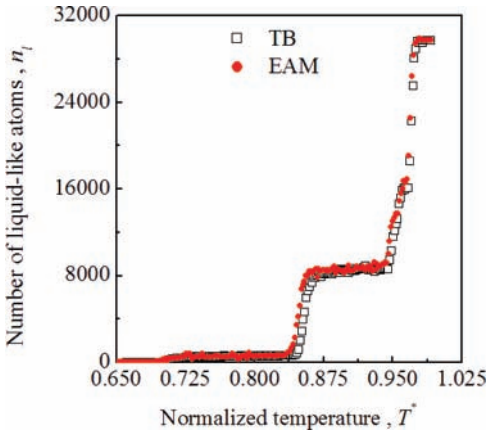

Figure 6. The number n_l of liquidlike atoms as a function of the normalized temperature T^* for simulations employing the TB and the EAM potential. A superposition of data is observed.

GB Diffusion

Simulation runs 4 ns long were carried out at constant temperature to characterize the dynamical behavior of atoms diffusing across partially molten GB regions. Only atomic species moving from external to internal surfaces and vice versa were considered. For each atom undergoing a successful GB diffusion event the time period τ over which diffusion across partially molten GBs took place was evaluated. The exact

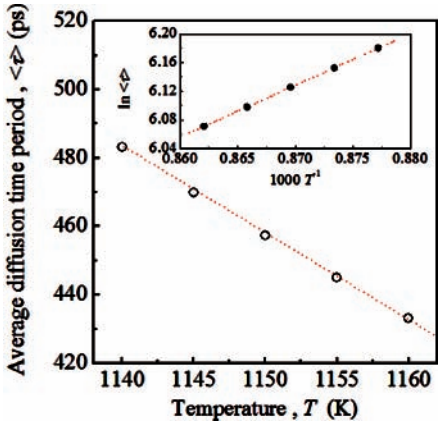

Figure 7. The average time period $\langle\tau\rangle$ of successful diffusion events at GBs as a function of the temperature T. A marked decreasing trend is observed. The $\ln\langle\tau\rangle$ is reported as a function of the inverse of temperature T^{-1} in the inset. The approximate linearity of the obtained plot indicates the exponential character of the dependence of $\langle\tau\rangle$ on T.

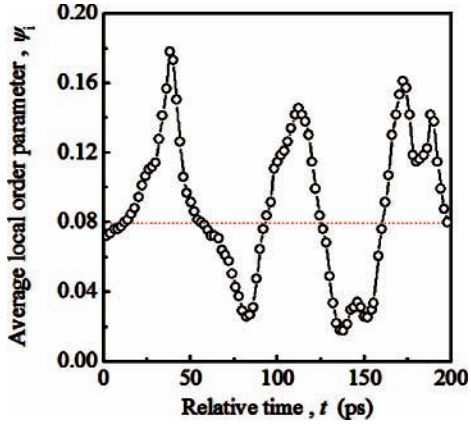

Figure 8. The average local order parameter $\bar{\psi}_i$ for an atom diffusing at GBs as a function of the time t. Time t is given on a relative scale for the sake of illustration. Data refer to a successful diffusion event from the internal surface to the external one across a GB region at 1150 K. $\bar{\psi}_i$ changes irregularly roughly between 0.02 and 0.16 in time intervals on the order of 30−40 ps. The horizontal dotted line marks the $\bar{\psi}_i$ threshold value at 0.08.

identification of the instants in which a diffusing atom leaves the free surface to enter the GB or, oppositely, leaves the GB emerging at the free surface is often relatively difficult. In most cases an arbitrary choice is necessary. The extent of arbitrariness introduced by such choice is however of only 30 to 70 fs, which leaves unaffected final results being time periods τ on the order of 300 ps. Within the framework discussed above, the time period τ provides a rough estimate of the rate of diffusion processes between external and internal surfaces. It should be noted that τ does not quantify the characteristic rate of single displacements between equilibrium sites but rather the average time interval required for a given atom to cover the diffusion path across GBs. The time period τ should therefore be regarded as the lifetime of a given diffusing atom in GBs. Accordingly, the shorter τ, the higher the diffusion rate across the disordered GB region.

The mean time period $\langle\tau\rangle$ was evaluated by averaging over the time periods τ underlying all the successful GB diffusion events observed. Calculations were performed at five different temperatures in the range between 1140 and 1160 K. The number of successful diffusion events allowing an atomic species to move from one hollow cube side to the other increases with temperature. Simulations specifically addressed to study the diffusion behavior were carried out in two stages.[46] An *NhT* run of 50 ps was used to bring the system to the desired thermodynamic state point by setting the temperature value. The system was successively relaxed for additional 50 ps in the *NVE* ensemble, i.e., at constant number of particles N, volume V, and energy E, to avoid the coupling with the stochastic heat bath and its effects on dynamics.[31,32,46] Each *NVE* calculation was carried out for 4 ns. The data reported in Figure 7 indicate that $\langle\tau\rangle$ decreases as the temperature T increases. Thus, the rate of diffusion across GBs increases with temperature according to general expectations. The dependence $\langle\tau\rangle$ on temperature T is relatively marked and apparently linear. However, a linear trend is also obtained by quoting $\ln\langle\tau\rangle$ as a function of T^{-1} as shown in the inset of Figure 7. This suggests for $\langle\tau\rangle$ an exponential dependence on temperature. An apparent activation energy E_a for the self-diffusion process of Au atoms across GBs amounting to about 60 kJ mol^{-1} can be obtained from the linear semilogarithmic plot in the inset of Figure 7. Such a value is much lower than the one of about 180 kJ mol^{-1} obtained from experimental investigation in bulk[47] but still far from the activation energy of about 35 kJ mol^{-1} for atomic diffusion processes in molten Au.[48] TB simulation values are not far from them. To further address this point, *NhT* and *NVE* simulations were carried out as previously described on an Au bicrystal consisting of about 39 000 atoms and containing an extended (110)×(110) twin boundary. The procedure followed to generate such structure according to the coincident-site-lattice method is described elsewhere.[49] The apparent diffusion coefficient D_{GB} was evaluated at the five above-mentioned temperature values by calculating the root-mean-square displacements[31] of atomic species in the neighborhood of the twin boundary. Data were arranged linearly in the semilogarithmic plot of $\ln D_{GB}$ as a function of T^{-1}, not reported here for the sake of brevity, allowing the estimation of an activation energy of about 106 kJ mol^{-1} for the GB diffusion processes. It follows that diffusion across partially molten GBs cannot be regarded as a conventional diffusion process in a molten phase but rather as intermediate between the diffusion in normal GBs and in liquid phases.

Such circumstances should be ascribed to the particular characteristics of liquidlike framework at GBs, which is roughly formed by a single atomic layer by each side of lateral neighboring domains. It is then on the average only two atoms thick, which is also the thickness value of molten layers at both external and internal (100) surfaces. Contrary to surface atoms, GB liquidlike atoms are however surrounded by solidlike atoms which do not permit a full relaxation of their strains. The mobility of GB liquidlike species is correspondingly affected. The dynamics of liquidlike atoms diffusing at GBs is governed by a continuous and irregular oscillation between liquid- and solidlike features. Data referring to a successful diffusion event from internal to external surfaces across a GB region are quoted in Figure 8, where the average local order parameter $\bar{\psi}_i$ of the diffusing atom is reported as a function of time t. It can be seen that $\bar{\psi}_i$ undergoes an irregular variation roughly between 0.02 and 0.16 in time intervals 30−40 ps long. It should be also noted that the $\bar{\psi}_i$ changes are quite definite, the identification of atomic dynamics as solid- or liquidlike being not merely a question of threshold values. Except for a few circumstances, the change of solid- or liquidlike character of atoms diffusing at GBs is therefore physically meaningful. On such a basis, it is relatively easy to identify differences between diffusion processes of liquidlikelike atoms at GBs and in liquid phases. Among the others, "solvent cages" seem to play an outstanding role. In liquid phases, each diffusing atom is surrounded by

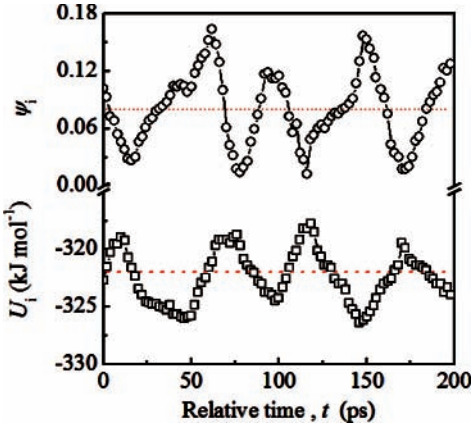

Figure 9. The local order parameter $\bar{\psi}_i$ and the potential energy U_i for a given atom i diffusing at GBs as a function of the time t. Time t is given on a relative scale for the sake of illustration. Data refer to an atomic configuration at 1155 K. A coupling between the character of atomic dynamics and the potential energy is observed. The horizontal dotted lines mark the $\bar{\psi}_i$ threshold value at 0.08 (upper line) and the average potential energy U of an Au bulk at 1155 K.

species with equivalent dynamic properties. Their irregular vibrations around approximate equilibrium sites and their occasional translational displacements when free volume becomes available in a neighboring position give rise to the well-known random walk underlying diffusion. In partially molten GB regions diffusing atoms are instead surrounded by only a few liquidlike neighbors, whereas the others possess solidlike character and are more or less rigidly connected to the bulk. Under such conditions, local energy fluctuations can significantly affect the character of atomic dynamics and determine the switch from solid- to liquidlike behavior and vice versa. A coupling between dynamics and potential energy of GB diffusing species has been actually observed. An example is given in Figure 9, where local order parameter $\bar{\psi}_i$ and potential energy U_i values are quoted as a function of time t for an atom i. Data point out that potential energy U_i fluctuations induce corresponding fluctuations in the average local order parameter $\bar{\psi}_i$. It is also worth noting that potential energy U_i fluctuations arise from a cooperative redistribution of kinetic energy on small ensembles of 15 to 20 atoms. The analysis of energy redistribution mechanisms among neighboring species presents however considerable difficulties and, being that it is also beyond the scope of the present work, was not pursued further.

An interesting point to note is that the thickness of liquidlike atomic layers at GBs becomes larger at triple junctions, where higher degrees of structural disorder are also observed. According to the Voronoi polyhedra space tessellation,[50] such regions are for example characterized by larger atomic volumes. The volume of species located at triple junctions is indeed approximately 14% larger than the one of atoms in GBs, which in turn is about 8% larger than that of bulklike atoms. The direct consequence on the diffusion behavior of liquidlike species is that diffusion rates are on the average about 20% larger than for other GB regions. Triple junctions can be thus regarded as particularly favored sites for atomic diffusion in partially molten GBs.

Observed GB diffusion events deserve here a final comment. The anomalous diffusion behavior at partially molten GBs is a result of their stability within the hollow nanocube. Even though subjected to local atomic rearrangements, GBs do not change in fact their position. This property is characteristic of GBs in nanometer-sized solids. In other cases, including nanostructured solid phases formed by neighboring coherent diffraction domains, GBs often undergo rotation and migration processes aimed at lowering their energy even at relatively low temperatures.[51,52] For example, a slow migration has been also observed in the Au bicrystal containing a twist boundary used to estimate the activation energy of diffusion events in extended GBs. Such processes are governed by mechanisms, based on so-called atomic "shuffling" events,[53,54] remarkably different from the ones observed in the present work. Involving each "shuffling" event small groups of atoms,[53,54] the occurrence of single atom thermally activated diffusion is of course prevented. Furthermore, it should be noted that the GB area in the nanocube considered is considerably small even compared to that of the usual nanostructured systems. Taking into account that the outer planes of both external and internal cube surfaces are molten, GB regions measure indeed on average only about 7×2 nm^2. Under such circumstances, melting is smeared over a relatively large temperature range. On the contrary, it is quite sharp for larger GB areas. The attainment of partial GB melting is therefore possible only in those systems in which single GB regions are small. As pointed out above, for single atomic diffusion events to occur GB regions must however be also stable. This restricts the possible occurrence of single atom diffusion in partially molten GBs to hollow nanometer-sized systems with wall thickness within a particular range. Thin walls would not be indeed able to withstand surface melting, whereas thick walls would lengthen the GB diffusion path thus lowering the probability of successful external−internal connection.[45]

It is finally worth mentioning that the finer details of diffusion processes at partially molten GBs are sensitive to the GB structure. Numerical simulations carried out on nanometer-sized hollow cubes with sides 8 nm long and walls 3 nm thick but (111) crystallographic facets, and then different GB structure, show indeed that the temperature range over which GBs melt is slightly smaller. Small changes in side length or wall thickness also result in slight modifications of GB melting quantitative features. This of course affects the diffusion behavior. The results obtained, not shown here for sake of brevity, indicate however that the anomalous diffusion still takes place even though at different temperatures.

Conclusions

The numerical findings obtained from molecular dynamics simulations indicate that the nanometer-sized Au hollow cube investigated is a heterogeneous system formed by sets of atoms with different coordination shells. Such heterogeneity deeply affects thermal response and melting behavior, the sets of atomic species undergoing melting within well distinct temperature ranges. Melting involves successively edge, surface, GB, and bulklike species. When GB regions are only partially molten, external and internal surfaces are already covered by a thin layer of molten phase. Under such circumstances, a percolating framework of atoms with liquidlike character connects the two sides of the hollow nanometer-sized structure. Liquidlike species are able to diffuse along such a preferential path and move across GBs, attaining external surfaces from hollow cube interior and vice versa. Within a relatively narrow temperature range suitable conditions therefore exist for connecting the two parts of the hollow structure and exchanging species between them.

Although the diffusion process across GBs involves atomic species with liquidlike character, its mechanism is substantially different from that of a free diffusion in liquid phase. Liquidlike GB atoms are indeed surrounded by solidlike ones which considerably affect their displacement. A major role is played by local energy redistribution processes. A coupling between

liquid- or solidlike character of atomic dynamics, atomic mobility across GB regions, and potential energy of diffusing species has been in fact observed. Preliminary results of the analyses aimed at characterizing the finer details of diffusion dynamics point out that diffusion across partially molten GBs is an intermittent cooperative process involving 1 to 0.2 of atoms. The apparent activation energy for a successful diffusion event leading a species to cross GB regions is intermediate between that of thermally activated diffusion in a liquid phase and that at solid GBs.

Further research work is needed to investigate the details of diffusion processes across GBs under different conditions. Experimental work on similar structures would also be extremely useful to ascertain the possible exploitability of such processes for promoting the interaction of chemical species contained in the hollow interior with the ones outside and vice versa.

Acknowledgment. Financial support has been provided by the University of Cagliari. A. Ermini, ExtraInformatica s.r.l. is gratefully acknowledged for his technical support.

References and Notes

(1) *Hollow and Solid Spheres and Microspheres: Science and Technology Associated with Their Fabrication and Application*; Wilcox, D. L. Sr., Berg, M., Bernat, T., Kelleman, D., Cochran, J. K., Jr., Eds.; MRS Proceedings Vol. 372, Materials Research Society: Pittsburgh, PA, 1994.
(2) Ozin, G. A.; Arsenault, A. C. *Nanochemistry. A Chemical Approach to Nanomaterials*; RSC Publishing: Cambridge, U.K., 2005.
(3) Mathlowitz, E.; Jacob, J. S.; Jong, Y. S.; Carino, G. P.; Chickering, D. E.; Chaturvedl, P.; Santos, C. A.; Vijayaraghavan, K.; Montgomery, S.; Bassett, M.; Morrell, C. *Nature* **1997**, *386*, 410.
(4) Huang, H.; Remsen, E. E.; Kowalewski, T.; Wooley, K. L. *J. Am. Chem. Soc.* **1999**, *121*, 3805.
(5) Xia, Y.; Halas, N. J. *MRS Bull.* **2005**, *30*, 338.
(6) Yao, H.; Takada, Y.; Kitamura, N. *Langmuir* **1998**, *14*, 595.
(7) Ung, T.; Liz-Marzan, L. M.; Mulvaney, P. *Langmuir* **1998**, *14*, 3740.
(8) Marinakos, S. M.; Novak, J. P.; Brousseau, L. C., III; House, A. B.; Edeki, E. M.; Feldhaus, J. C.; Feldheim, D. L. *J. Am. Chem. Soc.* **1999**, *121*, 8518.
(9) Fleming, M. S.; Mandal, T. K.; Walt, D. R. *Chem. Mater.* **2001**, *13*, 2210.
(10) Averitt, R. D.; Sarkar, D.; Halas, N. J. *Phys. Rev. Lett.* **1997**, *78*, 4217.
(11) Oldenburg, S. J.; Averitt, R. D.; Westcott, S. L.; Halas, N. J. *Chem. Phys. Lett.* **1998**, *288*, 243.
(12) Caruso, F.; Spasova, M.; Salgueirino-Maceira, V.; Liz-Marzan, L. M. *Adv. Mater.* **2001**, *13*, 1090.
(13) Sun, Y.; Xia, Y. *Science* **2002**, *298*, 2176.
(14) Sun, Y.; Mayers, B. T.; Xia, Y. *Nano Lett.* **2002**, *2*, 481.
(15) Sun, Y.; Xia, Y. *J. Am. Chem. Soc.* **2004**, *126*, 3892.
(16) Chen, J.; Wiley, B.; McLellan, J.; Xiong, Y.; Li, Z.-Y.; Xia, Y. *Nano Lett.* **2005**, *5*, 2058.
(17) Metraux, G. S.; Cao, Y. C.; Jin, R.; Mirkin, C. A. *Nano Lett.* **2003**, *3*, 519.
(18) Hao, E.; Li, S.; Bailey, R. C.; Zou, S.; Schatz, G. C.; Hupp, J. T. *J. Phys. Chem. B* **2004**, *108*, 1224.
(19) Yang, J.; Lee, J. Y.; Too, H.-P. *J. Phys. Chem. B* **2005**, *109*, 19208.
(20) Vasquez, Y.; Sra, A. K.; Schaak, R. *J. Am. Chem. Soc.* **2005**, *127*, 12504.
(21) Schwartzberg, A. M.; Olson, T. Y.; Talley, C. E.; Zhang, J. Z. *J. Phys. Chem. B* **2006**, *110*, 19935.
(22) Schwarz, U. S.; Safran, S. A. *Phys. Rev. E* **2000**, *62*, 6957.
(23) Huhtala, M.; Kuronen, A.; Kaski, K. *Comput. Phys. Commun.* **2002**, *146*, 30.
(24) Kang, J. W.; Hwang, H. J. *Nanotechnology* **2003**, *14*, 402.
(25) Moon, W. H.; Hwang, H. J. *Nanotechnology* **2004**, *15*, 431.
(26) Bilalbegovic, G. *Phys. Rev. B* **2004**, *70*, 045407.
(27) Tsai, P.-C.; Jeng, Y.-R.; Fang, T.-H. *Phys. Rev. B* **2006**, *74*, 045406.
(28) Wang, Z.; Zu, X.; Gao, F.; Weber, W. J. *J. Appl. Phys.* **2006**, *100*, 063503.
(29) Hasnaoui, A.; van Swygenhoven, H.; Derlet, P. M. *Phys. Rev. B* **2002**, *66*, 184112.
(30) Cleri, F.; Rosato, V. *Phys. Rev. B* **1993**, *48*, 22.
(31) Allen, M. P.; Tildesley, D. *Computer Simulations of Liquids*; Clarendon Press: Oxford, 1987.
(32) Qi, Y.; Çağin, T.; Johnson, W. L.; Goddard, W. A., III *J. Chem. Phys.* **2001**, *115*, 385.
(33) Morris, J. R. *Phys. Rev. B* **2002**, *66*, 144104.
(34) Morris, J. R.; Song, X. *J. Chem. Phys.* **2002**, *116*, 9352.
(35) Rosato, V.; Ciccotti, G.; Pontikis, V. *Phys. Rev. B* **1986**, *33*, 1860.
(36) Lutsko, J. F.; Wolf, D.; Phillpot, S. R.; Yip, S. *Phys. Rev. B* **1989**, *40*, 2841.
(37) Delogu, F. *Phys. Rev. B* **2006**, *73*, 184108.
(38) Barnett, R. N.; Landman, U. *Phys. Rev. B* **1991**, *44*, 3226.
(39) Hakkinen, H.; Manninen, M. *Phys. Rev. B* **1992**, *46*, 1725.
(40) Landa, A.; Wynblatt, P.; Hakkinen, H.; Barnett, R. N.; Landman, U. *Phys. Rev. B* **1995**, *51*, 10972.
(41) Jayanthi, C. S.; Tosatti, E.; Pietronero, L. *Phys. Rev. B* **1985**, *31*, 3456.
(42) Tartaglino, U.; Zykova-Timan, T.; Ercolessi, F.; Tosatti, E. *Phys. Rep.* **2005**, *411*, 291.
(43) Daw, M. S.; Baskes, M. I. *Phys. Rev. B* **1984**, *29*, 6443.
(44) Foiles, S. M.; Baskes, M. I.; Daw, M. S. *Phys. Rev. B* **1986**, *33*, 7983.
(45) Delogu, F. *Phys. Rev. B* **2007**, *75*, 235421.
(46) Donati, C.; Glotzer, S. C.; Poole, P. H.; Kob, W.; Plimpton, S. J. *Phys. Rev. E* **1999**, *60*, 3107.
(47) *Smithells Metals Reference Handbook*, 7th ed.; Brandes, E. A., Brook, G. B., Eds.; Butterworth-Heinemann: Oxford, 1992.
(48) Akhter, J. I.; Ahmed, E.; Ahmad, M. *Mater. Chem. Phys.* **2005**, *93*, 504.
(49) Delogu, F. *J. Phys.: Condens. Matter* **2007**, *19*, 396005.
(50) Finney, J. L. *Proc. R. Soc. London, Ser. A* **1970**, *319*, 495.
(51) *Materials Interfaces*; Wolf, D., Yip, S., Eds.; Chapman & Hall: London, 1992.
(52) Merkle, K. L.; Thompson, L. J.; Phillipp, F. *Interface Sci.* **2004**, *12*, 277.
(53) Zhang, H.; Srolovitz, D. J.; Douglas, J. F.; Warren, J. A. *Phys. Rev. B* **2006**, *74*, 115404.
(54) Lund, A. C.; Nieh, T. G.; Schuh, C. A. *Phys. Rev. B* **2004**, *69*, 012101.